Progress in Physics of Applied Materials 5 (2025), 117 – 123

Semnan University

Progress in Physics of Applied Materials

journal homepage: https://ppam.semnan.ac.ir/

Recyclable Ag-TiO_2 SERS Substrates Fabricated via Plasma Jet Printing

Mohammad Reza Abedi Jondani [a], Mahdi Shariat [a*], Eshrat Sadeghzadeh Lari [b]

[a] *Department of Physics, Faculty of Science, Vali-e-Asr University of Rafsanjan, Rafsanjan, Iran.*

[b] *Plasma and Nuclear Fusion Research School, Nuclear Science and Technology Research Institute (NSTRI), Box 14155-1339, Tehran, Iran.*

ARTICLE INFO

Article history:
Received: 11 April 2025
Revised: 25 Jun 2025
Accepted: 7 July 2025
Published online: 10 August 2025

Keywords:
Recyclable;
Surface-Enhanced Raman Scattering (SERS);
Ag-TiO_2 Nanocomposite;
Plasma Jet.

ABSTRACT

Recyclable surface-enhanced Raman scattering (SERS) substrates are important for real-world use because they can be used multiple times and are affordable. In this study, we developed a simple and low-cost method for fabricating recyclable SERS substrates by depositing silver nanoparticles onto TiO_2 nanostructures using an atmospheric pressure plasma jet without the need for chemical reducing or stabilizing agents. TiO_2 nanoparticles were synthesized via a sol-gel process and drop-cast onto glass substrates, followed by silver nanoparticle deposition through plasma jet printing. Structural analyses using XRD and FESEM confirmed the formation of anatase-phase TiO_2 and spherical Ag nanoparticles with tunable density. The SERS activity was optimized at a 60 s deposition time, and the substrates demonstrated strong plasmonic response and excellent reusability over five UV-assisted photocatalytic cleaning cycles using Rhodamine B and Methylene Blue. The substrates maintained over 80% of their initial Raman signal intensity, with no cross-contamination observed between analytes. These results show that the Ag-TiO_2 substrates are very sensitive, stable, and can be reused, making them a practical option for real-world SERS applications.

1. Introduction

Surface-enhanced Raman spectroscopy (SERS) is a highly sensitive technique that amplifies Raman scattering signals from molecules adsorbed onto rough metal surfaces. This enhancement can increase signal intensity by factors of 10^{10} to 10^{11}, enabling the detection of single molecules [1-5]. Common fabrication methods for SERS substrates include physical vapor deposition [6], electrochemical deposition [7], lithography [8], and self-assembly [9], each offering various structural configurations However, these techniques often suffer from significant drawbacks, such as high cost, time-consuming processes, and procedural complexity[10-13].

In recent years, plasma-based techniques have gained attention for the synthesis and deposition of nanomaterials. Plasma contains active species such as ions, electrons, free radicals, and high-energy photons, which facilitate low-temperature nanomaterial deposition via both chemical reactions and physical interactions [14]. Notably, free electrons in plasma can effectively reduce metal precursors, making this approach especially efficient. These features represent key advantages of plasma-based methods [15]. A new method for SERS substrate fabrication has been introduced by using atmospheric pressure plasma jet which offers several advantages over other methods, such as being cost-effective, easy to implement, and allowing for fast substrate preparation [16].

Atmospheric pressure plasma jets are used instead of traditional plasma deposition methods like non-equilibrium glow discharge plasma, which needs a vacuum and can only work with certain types, sizes, and shapes of objects. In contrast, atmospheric pressure plasmas based on arc discharge also present challenges, such as high thermal energy [17-20].

Plasma jets are capable of depositing various nanomaterials onto different substrates for SERS substrate

* Corresponding author. Tel.: +98-913-3903659
E-mail address: m.shariat@vru.ac.ir

Cite this article as:
Abedi Jondani M.R., Shariat M., and Sadeghzadeh Lari E., 2025. Recyclable Ag-TiO_2 SERS Substrates Fabricated via Plasma Jet Printing. *Progress in Physics of Applied Materials*, *5*(2), pp.117-123.DOI: **10.22075/PPAM.2025.37365.1145**

fabrication with minimal waste, as they do not require chemical reducing agents or stabilizers [21]. In a previous study, we deposited silver nanoparticles onto polyester fabric using a non-thermal plasma jet to create a SERS-active substrate. The substrate's performance was evaluated using Rhodamine B as the target molecule, achieving a sensitivity of 10^{-8} [14].

One of the ongoing concerns among scientists in the SERS field is the development of reusable substrates through regeneration, which is closely tied to the stability of the fabrication method. In recent years, researchers have focused on designing low-cost, robust, self-cleaning, recyclable, and reproducible nanostructured SERS substrates. However, achieving high sensitivity, recyclability, and reproducible SERS response remains challenging when using simple fabrication techniques. Due to their potential applications in areas such as environmental monitoring and human health, recyclable SERS substrates have become a major area of interest, as supported by several recent studies [22, 23].

Recently, the synthesis of semiconductor–noble metal SERS substrates has received significant attention due to the advantages mentioned above [24]. The development of recyclable SERS substrates composed of plasmonic nanostructures (such as Au or Ag) combined with semiconductor photocatalysts (including TiO_2, ZnO, WO_3, Fe_3O_4, CdS, Si, and others) has been widely reported in the literature [23-46].

TiO_2 has attracted considerable attention due to its chemical stability, non-toxicity, low cost, and other advantageous properties. It is commonly used as an anti-reflective coating in silicon solar cells and various optical thin-film devices. Additionally, TiO_2 is employed in catalytic reactions, where it acts as the catalyst and carries metals and metal oxides as drivers. The applications of titanium oxides depend strongly on their particle size and crystalline structure. Owing to its electrical, optical, and photocatalytic properties, TiO_2 has become a key material for nanoparticle research. Various synthesis methods have been employed to produce TiO_2 nanoparticles, including hydrothermal, mechanochemical, thermal plasma with radio frequency, sol-gel, and chemical vapor condensation techniques [1]. TiO_2 is considered a suitable candidate for use in heterogeneous catalysis. Its significance in practical applications stems from its resistance to harsh chemical environments and its stability under prolonged light exposure [47].

The sol-gel process is a widely used method for synthesizing solid materials, including nanoparticles, from small molecular precursors. It is particularly effective for producing metal oxides such as TiO_2. Compared to other synthesis techniques, the sol-gel method offers several advantages, including high purity, uniformity, compositional and stoichiometric control, low cost, ease of processing, flexibility in doping with high concentrations of impurities, and the ability to coat large or complex surfaces. Subsequent heat treatment or annealing is typically required to enhance the structural stability of the nanoparticles, promote condensation, and support seed growth [48].

Fengyan Ge et al. fabricated a flexible and recyclable SERS substrate by depositing Ag nanoparticles onto TiO_2-coated cotton fabric. Owing to the synergistic effect of the Ag–TiO_2 heterostructure and the high adsorption capacity of the cotton fabric, the substrate exhibited excellent sensitivity for detecting p-aminothiophenol at low concentrations. Moreover, the SERS performance was shown to be recoverable after 180min of UV illumination, attributed to the photocatalytic activity of the TiO_2 layer on the fabric surface [29].

Sathi Das et al. fabricated a porous Ag–TiO_2 film with a nanocage-like structure using simple and low-cost methods. The resulting film exhibited excellent SERS sensitivity, recyclability, and cost-effectiveness. Although the Ag film demonstrated strong growth, its distribution was non-uniform due to the mesoporous, cage-like morphology of the TiO_2 layer.

To evaluate recyclability, the SERS substrate was exposed to UV illumination for 130min. The researchers then used the reusable Ag–TiO_2 substrate to detect various concentrations of urea and found it to be highly sensitive, covering the clinically relevant range of blood urea levels[23].

In this study, TiO_2 nanoparticles were produced using the sol-gel process and coated onto a surface via the drop-coating method. Ag nanoparticles were subsequently deposited directly onto the TiO_2 layer from a single $AgNO_3$ precursor solution using a plasma jet.

The plasma jet facilitates the in-situ reduction of the precursor to silver nanoparticles without the need for additional chemical reducing or stabilizing agents. This approach eliminates the need for multi-step procedures such as filtration, centrifugation, and purification, which are commonly required in conventional nanoparticle synthesis methods. The resulting layer is reusable as a SERS substrate.

2. Materials and Methods

Titanium (IV) isopropoxide ($C_{12}H_{28}O_4Ti$), nitric acid (HNO_3), ethanol (CH_3CH_2OH), Rhodamine B ($C_{28}H_{31}ClN_2O_3$), methylene blue ($C_{16}H_{18}ClN_3S$), and silver nitrate ($AgNO_3$) were purchased from Merck and used without further purification. These reagents were employed to synthesize TiO_2 and prepare the precursor solution, which was subsequently deposited onto glass substrates. In this study, the sol-gel method was selected for TiO_2 production due to its advantages in metal oxide synthesis, including high purity, flexibility in doping at high concentrations, ease of processing, and low cost [47].

For the synthesis of TiO_2, in the first step, 30cc of absolute ethanol is added to 10 cc of Titanium (IV) Isopropoxide, and the solution is stirred for 60 min using a magnetic stirrer. Then, 3 cc of HNO_3 is mixed with 150 cc of deionized water and added dropwise over 4 hours to the Titanium (IV) Isopropoxide solution at a constant temperature to obtain a gel-like solution. This gel is then placed at 100°C for 24 hours. The resulting product is a yellow powder. Finally, the powder is baked at 400 °C for

4hours until it transforms into a white TiO_2 nanoparticle powder.

The glass substrates are thoroughly cleaned with acetone, ethanol, and deionized water to remove any contaminants before coating. Then, 10 mg of the produced TiO_2 nanoparticles are dispersed in 50cc of deionized water. A 10µl drop of this dispersion is placed on the glass substrate and dried in an oven at 70 °C. This process is repeated by adding another 10 drops to build up the desired TiO_2 nanoparticle layer on the glass. Using this method, a relatively thick TiO_2 nanoparticle layer, approximately 400nm thick, is formed on the glass surface, which serves as a substrate for the deposition of silver nanoparticles. Finally, a layer of Ag nanoparticles is deposited directly onto the TiO_2 nanoparticle layer using a plasma jet.

A layer of Ag nanoparticles is deposited directly on the surface of TiO_2 nanoparticles using the plasma jet. Fig. 1 shows the schematic of the plasma jet used in Ag nanoparticles coating.

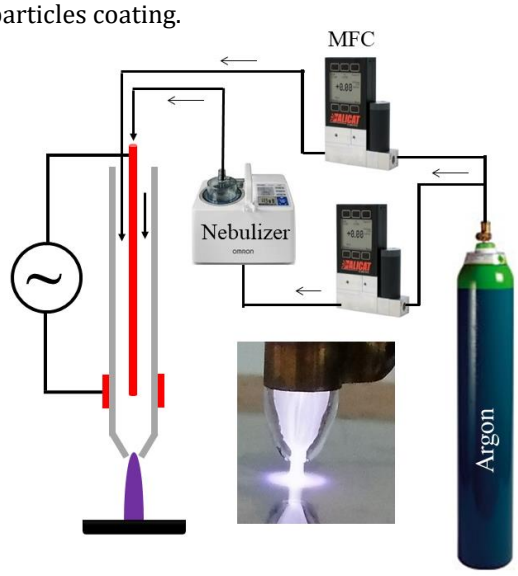

Fig. 1. Schematic and photograph of the plasma jet printing

This plasma jet operates in a dielectric barrier discharge (DBD) configuration. This jet includes two metal electrodes and a quartz tube (ID 6 mm and OD 8 mm) as a dielectric. The main electrode is a steel tube, through which an aerosol of silver precursor solution droplets is injected into the plasma. The ground electrode, a copper strip 1cm in width, surrounds the quartz tube and is placed 5mm from the end of the quartz nozzle. Argon gas with a flow rate of 2 SLPM is converted into plasma as it passes through the area between the two electrodes. The plasma power was calculated using a Lissajous method [49], and the measured value was 8.5 watts. The applied voltage was 7 kV. The plasma interacts with the precursor droplets, resulting in the deposition of Ag nanoparticles onto the substrate surface, which is positioned 3 mm away from the jet nozzle. The aerosol is produced from a silver precursor solution, which is injected into the plasma jet by an ultrasonic nebulizer (OMRON). This nebulizer contains 20 cc of a 24 mM silver nitrate solution in deionized water. Argon gas was used as the carrier gas and introduced into the nebulizer at a flow rate of 200 SCCM. It carried the precursor droplets through a stainless-steel tube into the generated plasma. The substrate was kept stationary under the plasma jet nozzle, and after 60 s of deposition, a black circular area with an approximate diameter of 2mm was formed.

X-ray diffraction (XRD) analysis and field emission scanning electron microscope (FESEM) imaging of the samples were performed using an X'Pert Pro device from Panalytical and a Sigma VP device from the German company ZEISS, respectively. Solutions of Rhodamine B (RhB) and methylene blue were prepared in ethanol at a concentration of 10^{-5}M. Then, 5µl of each solution was added to the samples for SERS analysis. A TakRam Raman spectrometer with a 532 nm wavelength, 20 mW output power, a 60× objective lens, and an integration time of 10 s was used to perform the SERS measurements. All measurements were conducted in triplicate, with standard deviations of reported spectral data remaining below 5%. To clean analytes from the surface of the SERS substrate for reuse, a 400 W UV lamp was employed. The lamp's irradiative power (~120 W), peak wavelength (365 nm), and irradiance at a distance of 10 cm (~95 mW/cm^2) were measured. The samples were positioned 10 cm away from the lamp during cleaning.

3. Results and Discussion

X-ray diffraction (XRD) analysis was performed to examine the crystal structure of the deposited layer on the glass substrate. As shown in Fig. 2, the XRD pattern of the deposited nanostructures exhibits characteristic peaks at 2θ = 25.27°, 37.73°, 48.01°, 54.30°, and 62.63°, corresponding to the (101), (004), (200), (105), and (204) crystal sheets of TiO_2, respectively. These peaks indicate that the nanoparticles predominantly exhibit the anatase phase, as referenced by (JCPDS21-1272). Although a few peaks related to the rutile phase are also observed, the anatase structure is clearly dominant. The Raman spectrum of TiO_2 (inset of Fig. 2) further supports the formation of the anatase phase, with characteristic peaks at 141, 193, 391, 516, and 637cm^{-1}. Given its superior photocatalytic properties, anatase-phase TiO_2 is considered a suitable material for the fabrication of reusable SERS substrates.

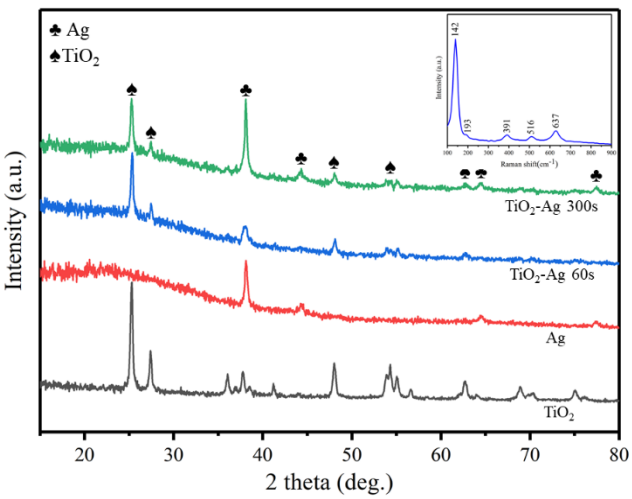

Fig. 2. XRD of TiO_2, Ag, and Ag-TiO_2 films at 60s and 300s, showing anatase TiO_2 and FCC Ag. (Inset: Raman confirming anatase TiO_2)

Additionally, peaks at 2θ = 38.13°, 44.35°, 64.5°, and 77.3° respectively corresponding to the (111), (200), (220), and (311) crystal sheets are observed for silver nanoparticles deposited on the glass substrate using a plasma jet. These peaks confirm the formation of Ag nanoparticles with a face-centered cubic (FCC) structure (JCPDS No. 04-0783). The XRD patterns of the Ag–TiO_2 composite layers display characteristic peaks corresponding to both TiO_2 and Ag crystal structures. The intensity of the Ag peaks increases with longer deposition times, indicating the growth of the silver layer on the surface of the TiO_2 particles. The crystallite size was estimated using the Debye–Scherrer equation. The TiO_2 nanocrystals in all layers exhibited sizes similar to those in the TiO_2 nanoparticle powder, approximately 29 nm. However, increasing the silver deposition time from 60 to 300s resulted in an increase in Ag nanocrystal size from approximately 20 to 30nm.

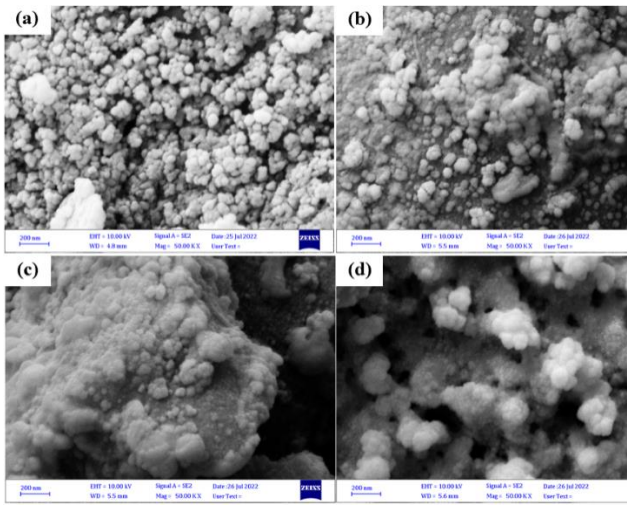

Fig. 3. FESEM images of (a) TiO_2 and Ag-TiO_2 films at deposition times of (b) 30s, (c) 60s, and (d) 300s

Fig. 3 shows the FESEM images of TiO_2 nanoparticles and the Ag-deposited TiO_2 surfaces at deposition times of 30, 60, and 300s. As observed in the images, both Ag and TiO_2 nanostructures appear approximately spherical. According to the XRD results, the particle sizes of Ag and TiO_2 are quite similar, making it difficult to distinguish between them in the FESEM images. It is evident that with increasing deposition time, the surface of the TiO_2 nanoparticles becomes increasingly covered by Ag nanoparticles. This trend is further supported by EDX analysis and EDX mapping, as shown in the corresponding images. The EDX data are summarized in Table 1.

The silver found in the EDX data comes from Ag nanoparticles, and the signals for oxygen and titanium show that TiO_2 nanomaterials are present. Since the ratio of oxygen to titanium stays the same in all samples, it can be said that the oxygen comes only from the TiO_2 structure, with no signs of other oxide phases in the layer (Table 1). Additionally, this oxygen-to-titanium ratio confirms that the anatase phase is present in the TiO_2 structure . However, in the sample where Ag was deposited for 300s, no detectable TiO_2 signal is observed, indicating that the surface is fully covered by silver nanoparticles.

EDX mapping in Fig. 4 illustrates that as the deposition time increases, the number of silver nanoparticles on the surface of the TiO_2 nanostructures also rises. As a result, the average distance between adjacent nanoparticles initially decreases. However, as the deposition time continues to increase, the nanoparticles start to clump together, which reduces the number of "hot spots" where the electromagnetic field is stronger for SERS.

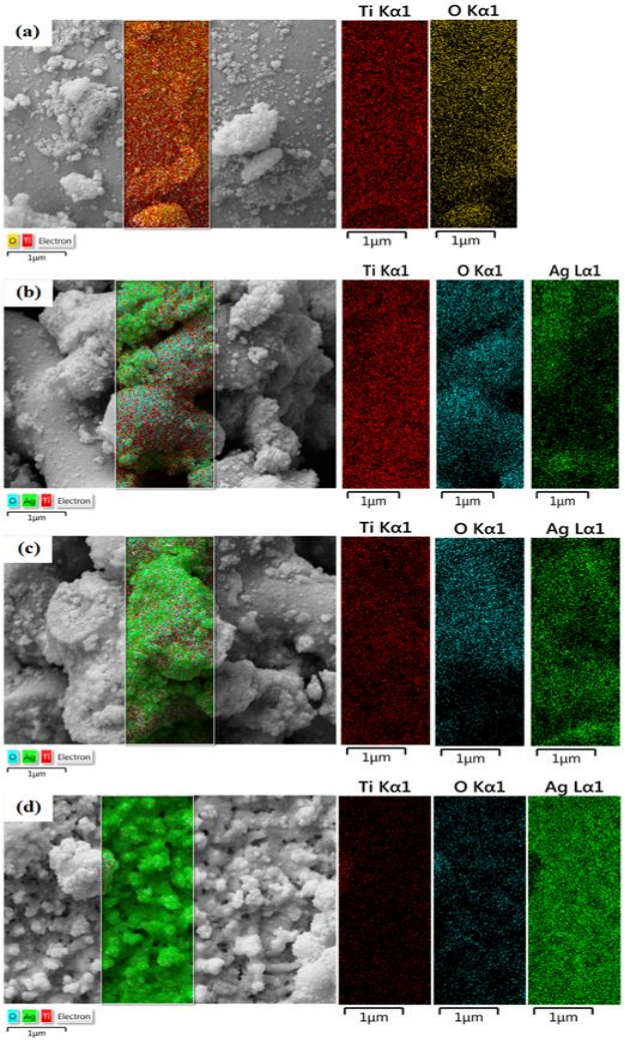

Fig. 4. EDX elemental mapping of (a) TiO_2 and Ag-TiO_2 films at deposition times of (b) 30s, (c) 60s, and (d) 300s

Fig. 5a displays the Raman spectra of RhB adsorbed on TiO_2 layers decorated with Ag nanoparticles at various deposition times (30, 60, 120, 180, and 300s).

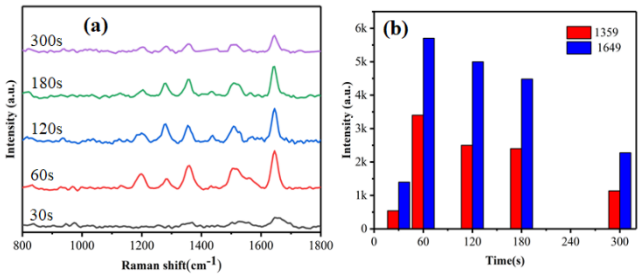

Fig. 5. (a) Raman spectra of 10^{-5} M RhB on Ag-TiO_2 at 30–300s Ag deposition; (b) Raman peak intensities of RhB at 1359 and 1649 cm^{-1}

The characteristic peaks of RhB are observed at 1149, 1276, 1359, 1508, 1529, and 1649cm^{-1}. As is also evident in Fig. 5b, the SERS signal intensity increases with deposition time, reaching a maximum at 60s. Beyond this point, further deposition leads to a gradual decrease in signal intensity. This trend is attributed to the interparticle distance of the Ag nanoparticles, which plays a key role in the SERS effect. According to the EDX mapping (Fig. 4), the density of Ag nanoparticles increases with deposition time, which indirectly indicates an increase in hot spot density up to the optimal time of 60s. However, at longer deposition times, the excessive density leads to nanoparticle agglomeration and clustering. This reduces the number of hot spots and, consequently, causes a drop in the SERS signal intensity. One important aspect of the Ag–TiO_2 substrates is that they can be reused because the TiO_2 matrix can break down the analyte molecules and refresh the substrate.

According to Fig. 6a, the photocatalytic degradation of RhB by the Ag–TiO_2 substrate under UV irradiation is clearly confirmed.

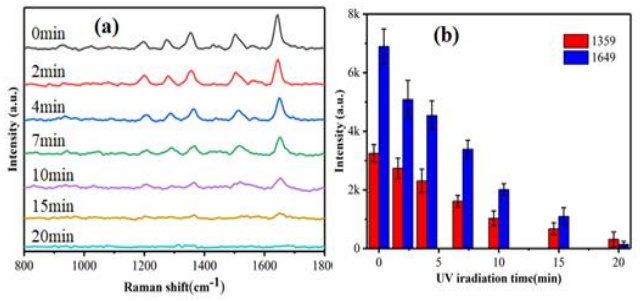

Fig. 6. (a) Raman spectra of RhB on Ag-TiO_2 under UV light; (b) Raman signal intensities of RhB at 1359 and 1649 cm^{-1} under UV light

The figure shows the evolution of the RhB Raman spectra on the Ag–TiO_2 surface at various UV exposure times. Furthermore, Fig. 6b shows the decreasing Raman signal intensity of two characteristic RhB peaks under 400W UV irradiation, indicating effective surface adsorption followed by photocatalytic degradation. As the irradiation time increases, the Raman signal intensity progressively decreases. After 20min of UV exposure, no detectable RhB peaks remain, indicating the effective removal of probe molecules from the surface of the Ag–TiO_2 substrate.

To verify the recyclability of the fabricated Ag–TiO_2 substrates, the identification and degradation cycle was repeated more than four times. In each cycle, the substrate was irradiated for 20 min, and the same initial concentration of RhB solution was reapplied to the surface (Fig. 7a). The TiO_2 substrates with silver nanoparticles made using a plasma jet show great ability to be reused, as seen in Fig. 7b. In the presence of RhB, the intensity of the 1649 cm^{-1} peak gradually decreased from 8049, 7516, 7343, 7129, to 6417 after the first to fifth photocatalytic degradation cycles, respectively. Although the intensity decreased to about 80% of its initial value after five UV irradiations, the signal remained sufficiently strong to allow for further measurements. The number of reuse cycles and the trend of SERS intensity reduction are comparable with similar studies [23, 24, 50]. These results confirm the recyclability, reusability, and practical applicability of the current SERS substrates.

Table 1. EDX data of Ag-TiO_2 films

	Ti	O	Ag
TiO_2	81.7	18.3	-
Ag-TiO_2 30s	61.4	13.9	25.7
Ag-TiO_2 60s	43.9	9.9	46.1
Ag-TiO_2 300s	1.5	1.7	96.8

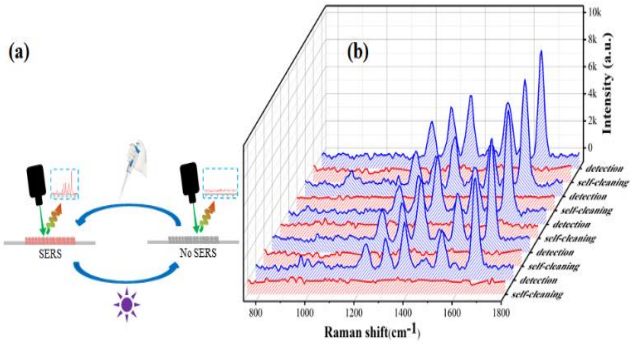

Fig. 7. (a) Schematic illustration of the recyclable substrate; (b) Raman spectra of 10^{-5} M RhB adsorbed onto Ag-TiO_2 in multiple cyclic detection and self-cleaning experiments

As shown in Fig. 8, after the detection and degradation of Rhodamine B on the Ag–TiO_2 substrate, the same substrate was reused to adsorb and detect methylene blue (MB).

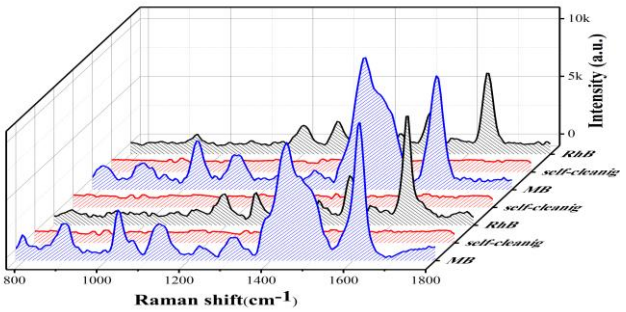

Fig. 8. Raman spectra of 10^{-5} M Rhodamine B and Methylene Blue in each 'detection-cleaning' cycle

Following UV-induced degradation of MB, RhB was once again introduced onto the same substrate for detection. This cycle of sequential detection and degradation was repeated multiple times under identical conditions. Notably, the TiO_2 layer coated with silver nanoparticles maintained nearly constant sensitivity throughout the process. Moreover, no Raman peaks associated with RhB were detected in the MB spectra, and vice versa, confirming complete degradation of the analytes and the absence of cross-contamination. These results highlight the excellent sensitivity and exceptional recyclability of the Ag–TiO_2 substrate, making it a promising low-cost platform for practical SERS applications.

4. Conclusions

Recyclable Ag–TiO_2 SERS substrates were fabricated by depositing silver nanoparticles onto TiO_2 nanostructures using an atmospheric pressure plasma jet. The TiO_2 nanostructures were synthesized via a simple sol-gel method and directly coated with silver nanoparticles through plasma-based deposition. XRD analysis confirmed the successful formation of the Ag–TiO_2 composite. FESEM imaging revealed the presence of silver nanoparticles on the TiO_2 surface and showed that the nanoparticle density could be tuned by adjusting the plasma deposition time. Thanks to the inherent photocatalytic properties of TiO_2, analyte molecules adsorbed on the substrate could be efficiently degraded. Specifically, RhB was completely removed from the substrate surface within 20 min of UV irradiation, enabling the SERS substrate to be reused for detecting other analytes. In future studies, plasma jet will be used for the direct deposition of TiO_2 nanostructures, which will enhance the scalability of the method. Additionally, optimizing plasma parameters is suggested to further improve SERS performance.

Funding Statement

The authors received no financial support for the research, authorship, and/or publication of this article.

Conflicts of interest

The authors declare that they have no known competing financial interests or personal relationships that could have appeared to influence the work reported in this paper.

Authors contribution statement

The authors confirm their contribution to the paper as follows: Study conception and design: Mahdi Shariat; Data collection: Mohammad Reza Abedi Jondani; Analysis and interpretation of results: Mahdi Shariat; Draft manuscript preparation: Eshrat Sadeghzadeh Lari and Mahdi Shariat. All authors critically reviewed the results and approved the final version of the manuscript.

References

[1] Xu, X., Li, H., Hasan, D., Ruoff, R.S., Wang, A.X. and Fan, D.L., 2013. Near-field enhanced plasmonic-magnetic bifunctional nanotubes for single cell bioanalysis. *Advanced Functional Materials*, *23*(35), pp.4332-4338.

[2] Blackie, E.J., Le Ru, E.C. and Etchegoin, P.G., 2009. Single-molecule surface-enhanced Raman spectroscopy of nonresonant molecules. *Journal of the American Chemical Society*, *131*(40), pp.14466-14472.

[3] Le Ru, E.C., Blackie, E., Meyer, M. and Etchegoin, P.G., 2007. Surface enhanced Raman scattering enhancement factors: a comprehensive study. *The Journal of Physical Chemistry C*, *111*(37), pp.13794-13803.

[4] Nie, S. and Emory, S.R., 1997. Probing single molecules and single nanoparticles by surface-enhanced Raman scattering. *science*, *275*(5303), pp.1102-1106.

[5] Le Ru, E.C., Meyer, M. and Etchegoin, P.G., 2006. Proof of single-molecule sensitivity in surface enhanced Raman scattering (SERS) by means of a two-analyte technique. *The journal of physical chemistry B*, *110*(4), pp.1944-1948.

[6] Durmanov, N.N., Guliev, R.R., Eremenko, A.V., Boginskaya, I.A., Ryzhikov, I.A., Trifonova, E.A., Putlyaev, E.V., Mukhin, A.N., Kalnov, S.L., Balandina, M.V. and Tkachuk, A.P., 2018. Non-labeled selective virus detection with novel SERS-active porous silver nanofilms fabricated by Electron Beam Physical Vapor Deposition. *Sensors and Actuators B: Chemical*, *257*, pp.37-47.

[7] Chen, S., Liu, B., Zhang, X., Mo, Y., Chen, F., Shi, H., Zhang, W., Hu, C. and Chen, J., 2018. Electrochemical fabrication of pyramid-shape silver microstructure as effective and reusable SERS substrate. *Electrochimica Acta*, *274*, pp.242-249.

[8] Kim, S.J., Hwang, J.S., Park, J.E., Yang, M. and Kim, S., 2021. Exploring SERS from complex patterns fabricated by multi-exposure laser interference lithography. *Nanotechnology*, *32*(31), p.315303.

[9] Wu, P.F., Fan, X.Y., Xi, H.Y., Pan, N., qian Shi, Z., You, T.T., Gao, Y.K. and Yin, P.G., 2022. Multifunctional self-assembled gold nanorod monolayer/Ti3C2Tx nanocomposites based on interfacial electrostatic for highly sensitive SERS detection of organic dyes and adenine. *Journal of Alloys and Compounds*, *920*, p.165978.

[10] Mekhilef, S., Saidur, R. and Kamalisarvestani, M., 2012. Effect of dust, humidity and air velocity on efficiency of

photovoltaic cells. *Renewable and sustainable energy reviews*, *16*(5), pp.2920-2925.

[11] Liu, H., Yang, L. and Liu, J., 2016. Three-dimensional SERS hot spots for chemical sensing: Towards developing a practical analyzer. *TrAC Trends in Analytical Chemistry*, *80*, pp.364-372.

[12] Liu, L.W., Zhou, Q.W., Zeng, Z.Q., Jin, M.L., Zhou, G.F., Zhan, R.Z., Chen, H.J., Gao, X.S., Lu, X.B., Senz, S. and Zhang, Z., 2016. Induced SERS activity in Ag@ SiO2/Ag core-shell nanosphere arrays with tunable interior insulator. *Journal of Raman Spectroscopy*, *47*(10), pp.1200-1206.

[13] Huang, Y., Xu, H., Yang, H., Lin, Y., Liu, H. and Tong, Y., 2018. Efficient charges separation using advanced BiOI-based hollow spheres decorated with palladium and manganese dioxide nanoparticles. *ACS Sustainable Chemistry & Engineering*, *6*(2), pp.2751-2757.

[14] Shariat, M., Karimipour, M. and Molaei, M., 2019. Influence of ambient gas on the optical properties of CdS quantum dots prepared by plasma-liquid interactions. *Journal of Luminescence*, *207*, pp.282-287.

[15] Hong, J., Yick, S., Chow, E., Murdock, A., Fang, J., Seo, D.H., Wolff, A., Han, Z., Van Der Laan, T., Bendavid, A. and Ostrikov, K.K., 2019. Direct plasma printing of nano-gold from an inorganic precursor. *Journal of Materials Chemistry C*, *7*(21), pp.6369-6374.

[16] Bajpai, A. and Sharma, R., 2020. Atmospheric pressure plasma jet: A complete tool for surface enhanced Raman spectroscopy substrates preparation. *Vacuum*, *172*, p.109033.

[17] Gandhiraman, R.P., Singh, E., Diaz-Cartagena, D.C., Nordlund, D., Koehne, J. and Meyyappan, M., 2016. Plasma jet printing for flexible substrates. *Applied Physics Letters*, *108*(12).

[18] Noeske, M., Degenhardt, J., Strudthoff, S. and Lommatzsch, U., 2004. Plasma jet treatment of five polymers at atmospheric pressure: surface modifications and the relevance for adhesion. *International journal of adhesion and adhesives*, *24*(2), pp.171-177.

[19] Stark, R.H. and Schoenbach, K.H., 1999. Direct current glow discharges in atmospheric air. *Applied Physics Letters*, *74*(25), pp.3770-3772.

[20] Hong, Y.C. and Uhm, H.S., 2006. Microplasma jet at atmospheric pressure. *Applied physics letters*, *89*(22).

[21] Shariat, M., 2023. Plasma jet printing of silver nanoparticles on polyester fabric as a surface-enhanced Raman scattering substrate. *Optik*, *277*, p.170698.

[22] Prakash, J., 2019. Fundamentals and applications of recyclable SERS substrates. *International Reviews in Physical Chemistry*, *38*(2), pp.201-242.

[23] Das, S., Saxena, K., Goswami, L.P., Gayathri, J. and Mehta, D.S., 2022. Mesoporous Ag–TiO2 based nanocage like structure as sensitive and recyclable low-cost SERS substrate for biosensing applications. *Optical Materials*, *125*, p.111994.

[24] Yang, W., Tang, J., Ou, Q., Yan, X., Liu, L. and Liu, Y., 2021. Recyclable Ag-deposited TiO2 SERS substrate for ultrasensitive malachite green detection. *ACS omega*, *6*(41), pp.27271-27278.

[25] Bright Ankudze, A.P. and Pakkanen, T.T., 2019. Ultrasensitive and recyclable superstructure of AueSiO2@ Ag wire for surface-enhanced Raman scattering detection of thiocyanate in urine and human serum. *Analytica Chimica Acta*, *1049*, p.179e187.

[26] Deng, C.Y., Zhang, G.L., Zou, B., Shi, H.L., Liang, Y.J., Li, Y.C., Fu, J.X. and Wang, W.Z., 2013. TiO2/Ag composite nanowires for a recyclable surface enhanced Raman scattering substrate. *Chinese Physics B*, *22*(10), p.106102.

[27] Du, J. and Jing, C., 2011. Preparation of Fe3O4@ Ag SERS substrate and its application in environmental Cr (VI) analysis. *Journal of Colloid and Interface Science*, *358*(1), pp.54-61.

[28] Fang, H., Zhang, C.X., Liu, L., Zhao, Y.M. and Xu, H.J., 2015. Recyclable three-dimensional Ag nanoparticle-decorated TiO2 nanorod arrays for surface-enhanced Raman scattering. *Biosensors and Bioelectronics*, *64*, pp.434-441.

[29] Ge, F., Chen, Y., Liu, A., Guang, S. and Cai, Z., 2019. Flexible and recyclable SERS substrate fabricated by decorated TiO2 film with Ag NPs on the cotton fabric. *Cellulose*, *26*(4), pp.2689-2697.

[30] Kandjani, A.E., Mohammadtaheri, M., Thakkar, A., Bhargava, S.K. and Bansal, V., 2014. Zinc oxide/silver nanoarrays as reusable SERS substrates with controllable 'hot-spots' for highly reproducible molecular sensing. *Journal of colloid and interface science*, *436*, pp.251-257.

[31] Kandjani, A.E., Mohammadtaheri, M., Thakkar, A., Bhargava, S.K. and Bansal, V., 2014. Zinc oxide/silver nanoarrays as reusable SERS substrates with controllable 'hot-spots' for highly reproducible molecular sensing. *Journal of colloid and interface science*, *436*, pp.251-257.

[32] Li, D., Li, D.W., Li, Y., Fossey, J.S. and Long, Y.T., 2010. Cyclic electroplating and stripping of silver on Au@ SiO 2 core/shell nanoparticles for sensitive and recyclable substrate of surface-enhanced Raman scattering. *Journal of Materials Chemistry*, *20*(18), pp.3688-3693.

[33] Liu, X.Y., Huang, J.A., Yang, B., Zhang, X.J. and Zhu, Y.Y., 2015. Highly reproducible SERS substrate based on polarization-free Ag nanoparticles decorated SiO2/Si core-shell nanowires array. *Aip Advances*, *5*(5).

[34] Liu, Y., Xu, C., Lu, J., Zhu, Z., Zhu, Q., Manohari, A.G. and Shi, Z., 2018. Template-free synthesis of porous ZnO/Ag microspheres as recyclable and ultra-sensitive SERS substrates. *Applied Surface Science*, *427*, pp.830-836.

[35] Sinha, G., Depero, L.E. and Alessandri, I., 2011. Recyclable SERS substrates based on Au-coated ZnO nanorods. *ACS applied materials & interfaces*, *3*(7), pp.2557-2563.

[36] Weng, X., Feng, Z., Guo, Y., Feng, J.J., Hudson, S.P., Zheng, J., Ruan, Y., Laffir, F. and Pita, I., 2016. Recyclable SERS substrates based on Fe 2 O 3–Ag hybrid hollow microspheres with crumpled surfaces. *New Journal of Chemistry*, *40*(6), pp.5238-5244.

[37] Xi, G., Yue, B., Cao, J. and Ye, J., 2011. Fe3O4/WO3 hierarchical core–shell structure: high-performance and recyclable visible-light photocatalysis. *Chemistry–A European Journal*, *17*(18), pp.5145-5154.

[38] Xu, S.C., Zhang, Y.X., Luo, Y.Y., Wang, S., Ding, H.L., Xu, J.M. and Li, G.H., 2013. Ag-decorated TiO 2 nanograss for 3D SERS-active substrate with visible light self-cleaning and reactivation. *Analyst*, *138*(16), pp.4519-4525.

[39] Yan, X., Wang, L., Qi, D., Lei, J., Shen, B., Sen, T. and Zhang, J., 2014. Sensitive and easily recyclable plasmonic SERS

substrate based on Ag nanowires in mesoporous silica. *Rsc Advances*, *4*(101), pp.57743-57748.

[40] Yang, J.L., Xu, J., Ren, H., Sun, L., Xu, Q.C., Zhang, H., Li, J.F. and Tian, Z.Q., 2017. In situ SERS study of surface plasmon resonance enhanced photocatalytic reactions using bifunctional Au@ CdS core–shell nanocomposites. *Nanoscale*, *9*(19), pp.6254-6258.

[41] Yang, X., Zhong, H., Zhu, Y., Shen, J. and Li, C., 2013. Ultrasensitive and recyclable SERS substrate based on Au-decorated Si nanowire arrays. *Dalton Transactions*, *42*(39), pp.14324-14330.

[42] Zhai, Y., Zhai, J., Wang, Y., Guo, S., Ren, W. and Dong, S., 2009. Fabrication of iron oxide core/gold shell submicrometer spheres with nanoscale surface roughness for efficient surface-enhanced Raman scattering. *The Journal of Physical Chemistry C*, *113*(17), pp.7009-7014.

[43] Zhang, C.X., Liu, L., Jun Yin, H., Fang, H., Mei Zhao, Y., Jian Bi, C. and Jun Xu, H., 2014. Recyclable surface-enhanced Raman scattering template based on nanoporous gold film/Si nanowire arrays. *Applied Physics Letters*, *105*(1).

[44] Zhang, M., Zhao, A., Wang, D. and Sun, H., 2015. Hierarchically assembled NiCo@ SiO 2@ Ag magnetic core–shell microspheres as highly efficient and recyclable 3D SERS substrates. *Analyst*, *140*(2), pp.440-448.

[45] Zhou, Y., Chen, J., Zhang, L. and Yang, L., 2012. Multifunctional TiO2-Coated Ag Nanowire Arrays as Recyclable SERS Substrates for the Detection of Organic Pollutants. *European Journal of Inorganic Chemistry*, *2012*(19), pp.3176-3182.

[46] Zou, X., Silva, R., Huang, X., Al-Sharab, J.F. and Asefa, T., 2013. A self-cleaning porous TiO 2–Ag core–shell nanocomposite material for surface-enhanced Raman scattering. *Chemical Communications*, *49*(4), pp.382-384.

[47] Carp, O., Huisman, C.L. and Reller, A., 2004. Photoinduced reactivity of titanium dioxide. *Progress in solid state chemistry*, *32*(1-2), pp.33-177.

[48] Ibhadon, A.O. and Fitzpatrick, P., 2013. Heterogeneous photocatalysis: recent advances and applications. *Catalysts*, *3*(1), pp.189-218.

[49] Hołub, M., 2012. On the measurement of plasma power in atmospheric pressure DBD plasma reactors. *International Journal of Applied Electromagnetics and Mechanics*, *39*(1-4), pp.81-87.

[50] Wu, H.Y., Lin, H.C., Liu, Y.H., Chen, K.L., Wang, Y.H., Sun, Y.S. and Hsu, J.C., 2022. Highly sensitive, robust, and recyclable TiO2/AgNP substrate for SERS detection. *Molecules*, *27*(19), p.6755.